Food Chemistry: X 21 (2024) 101054

Contents lists available at ScienceDirect

Food Chemistry: X

journal homepage: www.sciencedirect.com/journal/food-chemistry-x

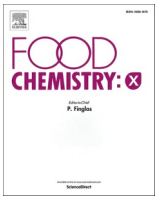

A paper-based ratiometric fluorescent sensor for NH_3 detection in gaseous phase: Real-time monitoring of chilled chicken freshness

Huang Xiaowei [a,b], Zhao Wanying [a], Sun Wei [a], Li Zhihua [a,*], Zhang Ning [a], Shi Jiyong [a], Zhang Yang [a], Zhang Xinai [a], Shen Tingting [a], Zou Xiaobo [a,c,*]

[a] School of Food and Biological Engineering, Jiangsu University, 301 Xuefu Rd., 212013 Zhenjiang, Jiangsu, China
[b] Focusight (Jiangsu) Technology Co., LTD, o.258-6 Jinhua Road, Wujin Economic Development Zone, 213146 Changzhou, Jiangsu, China
[c] International Joint Research Laboratory of Intelligent Agriculture and Agri-products Processing (Jiangsu University), Jiangsu Education Department, China

ARTICLE INFO

Keywords:
Ratio fluorescence
Visual analysis
Chilled Chicken Freshness
Paper-based sensors
Ammonia

ABSTRACT

A ratiometric fluorescence sensor platform with easy-to-use and accurate is nanoengineered for NH_3 quantitative detection and visual real-time monitoring of chicken freshness using smartphones. The ratiometric fluorescent probe formed by combining the zinc ion complex and carbon dots has a double-emitted fluorescence peak. The fluorescence intensity of the complex changed can be clearly observed with the increase of the concentration of ammonia solution under 365 nm wavelength excitation. In order to detect NH_3 concentration in gaseous phase, a portable paper-based sensor was designed. The sensor had a good linear relationship with NH_3 concentration ranging from 10.0 to 90.0 μmol/L and the LOD value was 288 nM. This fluorescent paper-based sensor was used to check the freshness of chicken breast refrigerated at 4 °C, revealed observable shifts from blue to green. The fluorescent paper-based sensor can detect NH_3 concentration in real time and simplify the monitoring process of meat freshness while ensuring accuracy and stability.

1. Introduction

In recent years, global chicken sales have increased by years. Because of its high protein content and low-fat content, chicken meat is very in line with the needs of modern people for a healthy diet. Chicken has become one of the main sources of meat consumption(P. Y. Li, Rao, Wang, & Hu, 2022). People's requirements for chicken quality and safety are also getting higher and higher(Z. Jia, Luo, Wang, Dinh, Lin, Sharma, et al., 2021; Kim, Park, Kim, & Shin, 2022; Kuswandi, Jayus, Oktaviana, Abdullah, & Heng, 2014; Lu, Yang, Liu, Liu, Ma, Wu, et al., 2020). To cater to consumers' demand for information about the freshness of chicken meat, the freshness indicator label is more and more concerned by the researchers as it can provide consumers with indicators of chicken freshness intuitively and quickly. At present, the most widely studied is the application of colorimetric sensing membranes based on pH changes in meat freshness indicators(Lee, Baek, Kim, & Seo, 2019; Lee, Park, Baek, Han, Kim, Chung, et al., 2019; Mastnak, Mohr, & Finsgar, 2023). The basic principle of colorimetric sensing membranes is that, as the meat degrades, protein is degraded by enzymes and microorganisms, along with, the production of nitrogenous volatile compounds, total volatile base nitrogen (TVB-N), which includes ammonia, dimethylamine, trimethylamine, and other substances (Qin, Ke, Faheem, Ye, & Hu, 2023; Wojnowski, Namiesnik, & Plotka-Wasylka, 2019). Levels of TVBN gradually shift the atmosphere within the package toward alkaline conditions as meat rotting rises, and the use of pH-based colorimetric sensing films can detect these changes.(Mastnak, Mohr, & Finsgar, 2023; Y. Sun, Zhang, Adhikari, Devahastin, & Wang, 2022). However, acid-base neutralization also occurs. Such as, chicken is easily infected by Salmonella, which metabolizes protein to produce acidic H_2S etc.(Chen, Ding, Zhu, Guo, Tang, Xie, et al., 2023; Lu, et al., 2020; Rosniawati, Rahayu, Kusumaningrum, Indrotristanto, & Nikastri, 2021). This causes acid-base neutralization of the headspace gas, so evaluating chicken freshness from changes in headspace gas pH alone could result in errors (see Fig. 1).

Usually, volatile compounds such as NH_3, TMA, DMA etc. are considered as total volatile basic nitrogen (TVB-N). Among these substances, NH_3 has the most considerable odor-release strength, produced as a result of the destructive activities of microorganisms and is considered one of the most important freshness indicators to monitor the quality and safety of meat products (Cai, Song, Zhang, Wang, Jian, Xu,

* Corresponding authors at: School of Food and Biological Engineering, Jiangsu University, 301 Xuefu Rd., 212013 Zhenjiang, Jiangsu, China (Zou Xiaobo).
E-mail addresses: lizh@ujs.edu.cn (L. Zhihua), zou_xiaobo@ujs.edu.cn (Z. Xiaobo).

https://doi.org/10.1016/j.fochx.2023.101054
Received 11 July 2023; Received in revised form 20 November 2023; Accepted 5 December 2023
Available online 9 December 2023

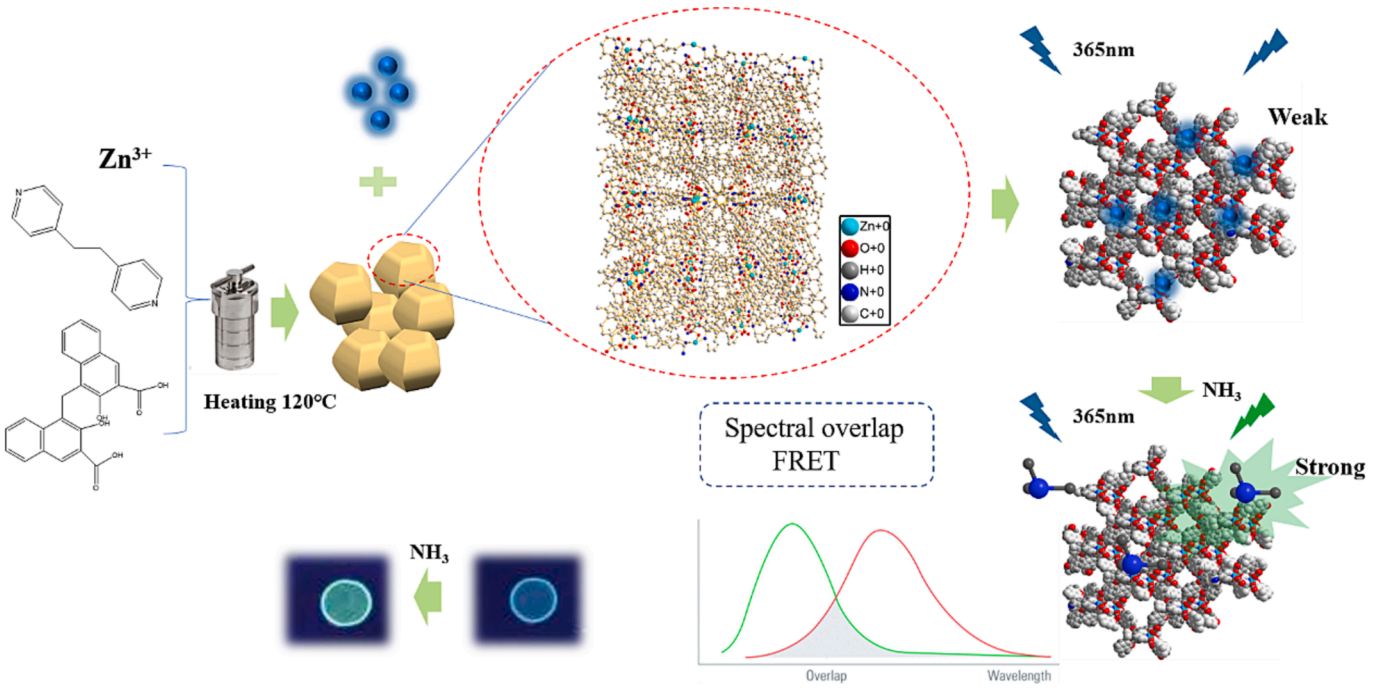

Fig. 1. Schematic diagram of Zn(PA) @CNQDs synthesis process and detection.

et al., 2022; Jiao, Sun, Hui, Dong, Li, Hui, et al., 2022; Meng, Luo, Dong, Zhang, He, Long, et al., 2020; Moosavi-Nasab, Khoshnoudi-Nia, Azimifar, & Kamyab, 2021; Rosniawati, Rahayu, Kusumaningrum, Indrotristanto, & Nikastri, 2021). So NH_3 was selected as target objects as chicken freshness indicators in this study. Due to the high requirement for timeliness and non-destruction in detecting the freshness of chicken (Mastnak, Mohr, & Finsgar, 2023). The development of an extremely sensitive and focused sensor for the online detection of ammonia gas in chilled chicken is crucial. An electronic nose is the most common method for rapid non-destructive testing of gases(Luo, Zhu, Lv, Wu, Yang, Zeng, et al., 2023). However, electronic noses based on metal oxide gas sensors need to work at high temperatures and are not suitable for chicken freshness detection. Visible light colorimetric technology is the most intuitive NH_3 gas visualization detection method(W. Y. Li, Sun, Liu, Rotaru, Robeyns, Singleton, et al., 2022), but it cannot avoid errors caused by environmental light interference. Infrared spectroscopy is also can be used for NH_3 gas analysis(Xiao, Sui, Yu, Chen, Yin, & Ju, 2019), however, it is susceptible to ambient humidity. The storage and transportation environment of cold fresh chicken is humid, low temperature, and dim, so these detection methods are difficult to use for real-time online monitoring of chicken freshness. Among these detection methods, fluorescence detection of NH_3 is simpler and more convenient (Mallick, Chandra, & Koner, 2016; E. S. Zhang, Hou, Yang, Zou, & Ju, 2020). Zhang et al.(J. Zhang, Xu, Shi, & Yang, 2021) proposed a highly selective NH_3 detection sensing strategy based on N, S CO-doped carbon dots (N, S-CDs). The prepared N, S-CDs exhibited excellent photoluminescence performance and fluorescence stability, while N, S-CDs exhibited fluorescence quenching in a wide linear range in the presence of 2–80 mmol/L NH_3 concentration. Sun et al.(L. Sun, Rotaru, & Garcia, 2022) designed a new high-performance gas colorimetric material based on a porous Fe (II) complex for detecting NH_3. It performs simple color recognition through smartphones, real-time monitoring and in situ evaluation of meat freshness. Jia et al.(R. Jia, Tian, Bai, Zhang, Wang, & Zhang, 2019) designed a cellulose-based proportional fluorescent material and proposed a visualization method for monitoring the freshness of seafood. The prepared proportional fluorescent material has a fast and reversible response to ammonia gas. These fluorescent probes have a good response to ammonia gas, but there are also some problems in practical applications. For example, the synthesis process of organic probes is very complex, which brings great difficulties to the actual preparation process. The complex volatile components of chicken require a high selectivity of the probe, and the relatively low concentration of ammonia produced by chicken requires a high sensitivity of the probe. In addition, some probes even operate in the "off" state with relatively low sensitivity.

In this study, the coordination polymers (CPs) were used as sensors to obtain complexes with different properties with stable, porous three-dimensional structures by combining different metal ions with different organic ligands(Lü, Chen, Li, Wang, Müllen, & Yin, 2019). However, the properties of coordination polymers formed by the combination of different metal ions and organic ligands are different, so designing CPs capable of detecting organic amines is challenging. Compared with single fluorescence emission, ratiometric fluorescent probes show better self-calibration(J. Wang, Li, Ye, Qiu, Liu, Huang, et al., 2021). Therefore, a solid-state sensor with Zn(PA)@CNQDs composite coordination polymer was designed as the probe to detect fatty amine gases. The electron-rich amine gas combines with the functional site on the surface of CPs to turn on the fluorescence of the polymer, and the purpose of detecting amines is achieved under the dual emission fluorescence signal of Zn(PA) and CNQDs.

Materials and methods

2.1. Chemicals and materials

$Zn(NO_3)_2{\cdot}6H_2O$, DMF, bis(4-pyridyl)ethane, ultrapure water, KOH, ammonia, sodium citrate, ammonium chloride, acetone, sodium sulfide, methanol, ethanol, isopropanol, ethane, cyclohexane, trichloroethane, ethylene all reagents do not require further purification.

2.2. Preparation of Zn(PA) (BPE) @CNQDs

The synthesis of CNQDs is as follows: ammonium chloride (0.53 g), sodium citrate (0.1 g), and water (5 ml) are mixed, added to a Teflon aluminum autoclave, and then heated to 180 °C for 4 h before being left at ambient temperature to allow for natural cooling. To get rid of non-

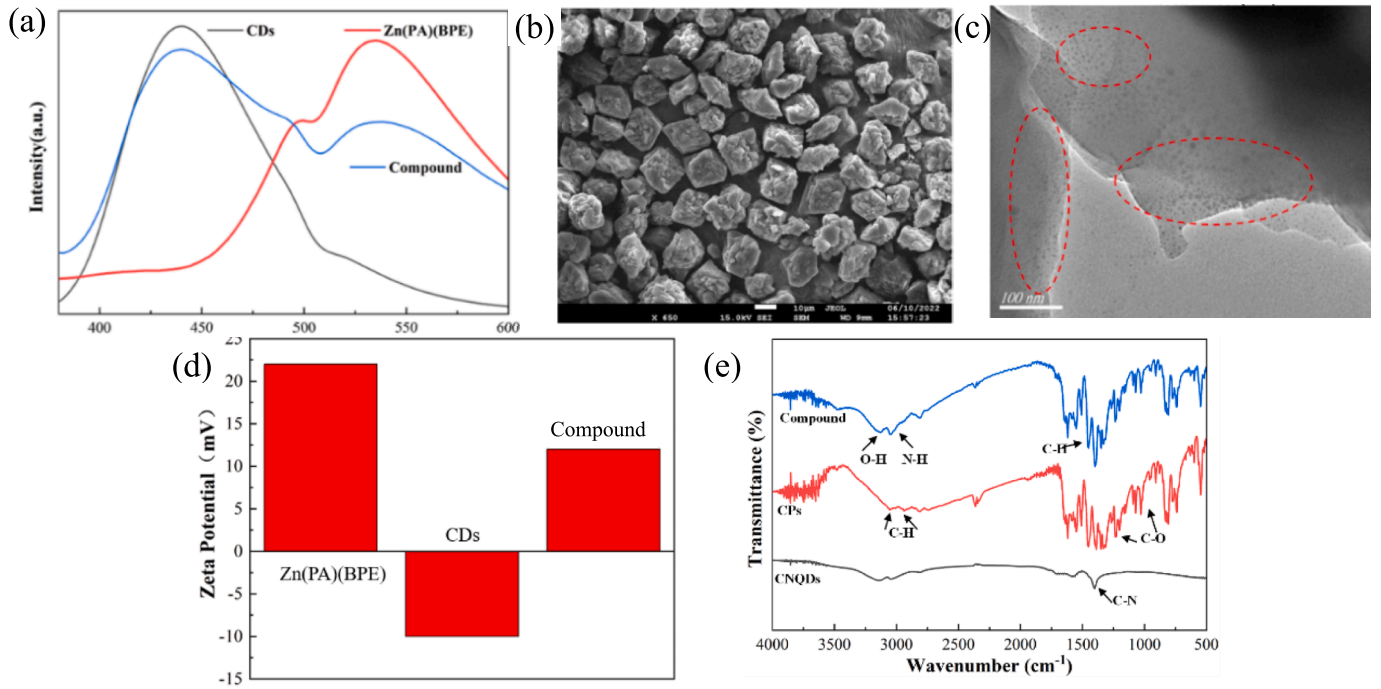

Fig. 2. (a) CDs, Zn(PA)(BPE) and complex fluorescence spectra; (b) Scanning electron microscopy of the complex; (c) Transmission electron microscopy of the complex; (d) CDs, Zn(PA) (BPE), and complex Zeta potential maps; (e) CDs, Zn(PA) (BPE), and composite mid-infrared spectra.

reactive precursors, the mixture is filtered on a 1000 Da dialysis membrane after freezing. Keep at 4 °C with the purified CNQDs solution after centrifuging the final product for 5 min at 8,000 rpm to get rid of any large, insoluble particulates.

Zn(PA)(BPE) @CNQDs synthesized according to the following method: 0.8 mmol $Zn(NO_3)_2{\cdot}6H_2O$ was mixed and stirred with 8 ml to obtain solution A, and 0.4 mmol bis(4-pyridyl)ethane was mixed with 0.8 mmol of bis(4-pyridyl)ethane with 40 ml ultrapure water to obtain solution B. Adjust the pH of solution B to 8 with 1 M KOH, mix solution A and solution B, and then put it into an autoclave for 5 min and heat it at 120 °C for 3 days to obtain a solid powdery substance. Vacuum freeze-dried for 2 days to obtain solid powder Zn (PA) (BPE), then take 3 mg CPs dissolved in ultrapure water mixed with 100 μl CNQD, stand for 1 h and centrifuge to wash off the supernatant to dissolve the mixture in 4 ml of ultrapure water again.

2.3. Zn(PA) @CNQDs complex for detection of ammonia

Ammonia was configured to react with the configured Zn(PA) @CNQDs complexes with different concentration gradients, and the concentrations of the complexes were optimally selected according to the supporting information. The emission peak intensity at 440 nm and 540 nm was recorded under wavelength excitation at 365 nm, and all relevant measurements were performed 3 times.

2.4. Detection of total nitrogen content in chicken breast (TVB-N)

Fresh chicken breasts were provided by a local slaughter plant (Fengyuan Co., Zhenjiang, China) within one hour after slaughter in insulated polystyrene boxes on ice. A Kjeldahl nitrogen analyzer was used to detect TVB-N in chicken breast. First, a 10 g chicken breast sample was homogenized with 75 ml ultrapure water. Next, 1 g MgO was added to the mixture utilized to eliminate the fundamental nitrogenous compounds from the chicken breast sample, which were then distilled off and absorbed via boric acid. The nitrogen concentration was then determined by mixing the mixture with 0.1 mol/L HCl. The TVB-N content in chicken breast samples was measured every 24 h, and the TVB-N content was calculated as follows:

$$X = \frac{(V_1 - V_2) \times C \times 14}{m} \times 100 \quad (1)$$

where X is the content of TVB-N in chicken breast, the unit is mg/100 g; m is the weight of the chicken breast sample, in g; V_1 is the volume of HCl consumed by the sample in ml; V_2 is the volume of HCl consumed by the contrast agent in ml; C is the concentration of HCl in M.

2.5. Preparation of portable ratiometric fluorescence sensors

The 7.5 mg/128 ml complex was dissolved in 2 ml of ultrapure water, the mixture was placed in a 10 ml centrifuge tube after uniform shaking, 20 μl of sample was dropped on qualitative filter paper, and a solid paper-based sensor was obtained after nitrogen blowing for 10 min. Finally, the sensor is placed in a sealed gas generator and different concentrations of ammonia solution are injected to react with the sensor. The change in the RGB value of the sensor is observed by the UV four-purpose analyzer, and its value is recorded with a smartphone (Huawei P40). The distribution of ammonia in the liquid and gas phases was analyzed, the volatilization of ammonia gas from various volumes of ammonia aqueous solution was estimated, and the precise calculation method was presented in the accompanying information. The standard concentration of ammonia gas is generated as follows: Dry fluorescent paper-based sensors are placed in homemade gas generators. Different concentrations of aqueous ammonia solutions are added to the sample cell, and ammonia is partially ionized in the water and volatilized into the air (H. Wang, Cui, Arshad, Xu, & Wang, 2018).

$$NH_3 \bullet H_2O \leftrightarrow NH_4^+ + OH^- K_a$$

$$\mathrm{P}(NH_3,\ \mathrm{g}) = K_B \bullet C_{BX} \quad (2)$$

Where $P(NH_3,g)$ is partial pressure of gaseous ammonia, K_B is Henry's constant 0.297 Pa(H_2O in Water, 298.15 K), C_{BX} is molar concentration of NH_3 mol/ L.

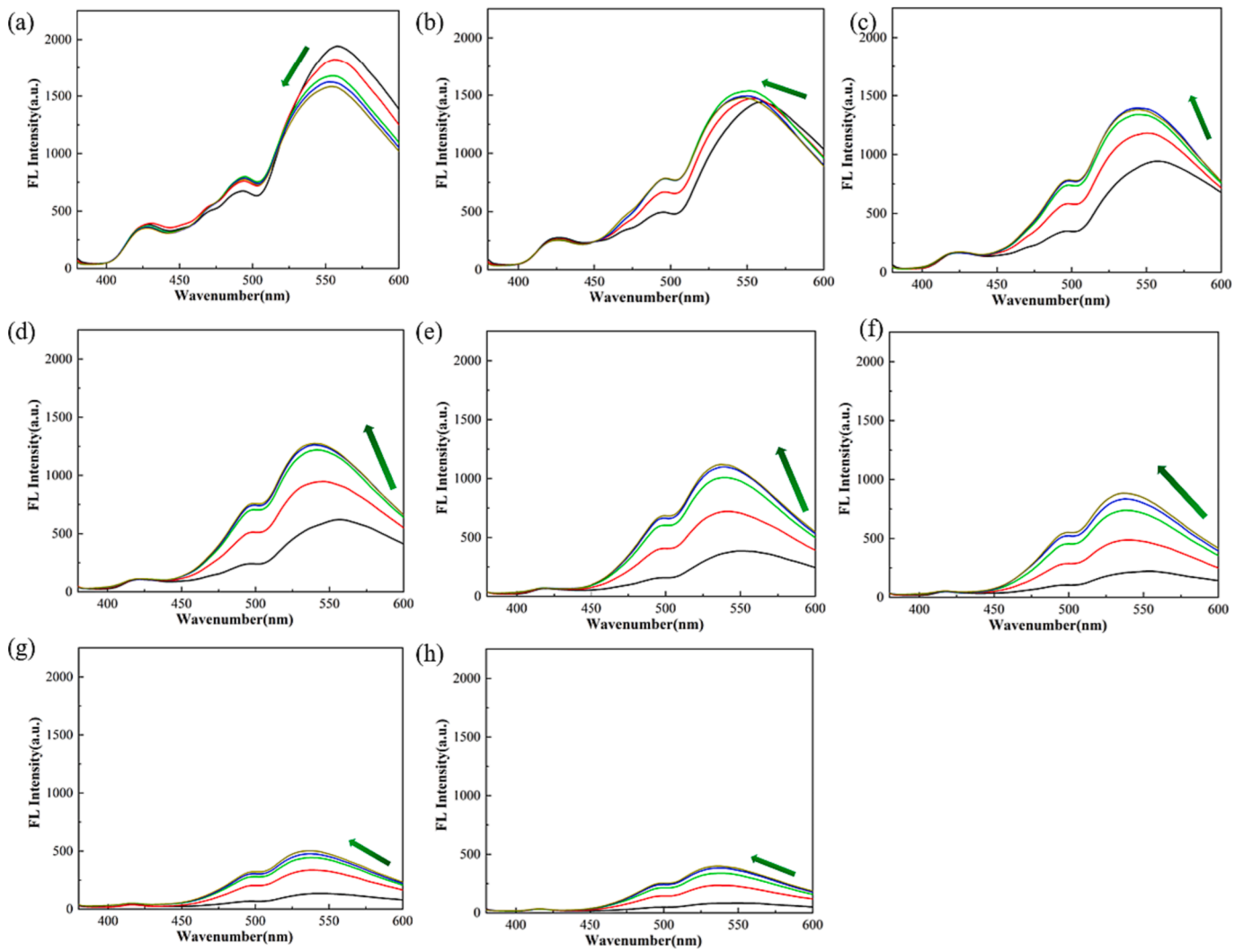

Fig. 3. Plotting of fluorescence intensity of Zn(PA)(BPE) complexes at different concentrations over time at 0.1 M ammonia concentration. (a) 1.5 mg/ml; (b) 1.5 mg/2ml; (c) 1.5 mg/4ml; (d) 1.5 mg/8ml; (e) 1.5 mg/16 ml; (f) 1.5 mg/32 ml; (g) 1.5 mg/64 ml; (h)1.5 mg/128 ml.

$$\mathrm{P}(NH_3,\mathrm{g}) = \frac{n(NH_3,\mathrm{g}) \bullet R \bullet T}{v(NH_3,g)} \tag{3}$$

Where $v(\mathrm{NH_3,g}) = 0.3927$ L, which was the volume of the sealed flask used in the home-built NH_3 generator, $R = 8.314$ J/(mol•K), $T = 298.15$ K, $\mathrm{M(H_2O)} = 18$ g/mol, $\mathrm{M(NH_3)} = 34$ g/mol, $n(\mathrm{NH_3,g})$ is the amount of ammonia in the gaseous state.

$$C_{B,x} = \frac{n(NH_3,l)}{n(NH_3,l) + n(H_2O)} \tag{4}$$

$$n_0(NH_3 \bullet H_2O) = \mathrm{n}(NH_3,\mathrm{g}) + \mathrm{n}(NH_3,l) + \mathrm{n}\left(NH_4^+\right) + \mathrm{n}(\mathrm{OH}^-) \tag{5}$$

Where $n_0(\mathrm{NH_3{\cdot}H_2O})$ is the amount of ammonia in the H_2O in the initial state, n $(\mathrm{NH_3},l)$ is the amount of ammonia in the liquid state, n $(\mathrm{H_2O})$ is the amount of H_2O, n $(\mathrm{NH_4^+})$ is the amount of NH_4^+, n $(\mathrm{OH^-})$ is the amount of OH^-. On basis of the equation (1) (2) (3) (4),

$$\mathrm{P} = \frac{n(NH_3,\mathrm{g}) \bullet R \bullet T}{V(NH_3,\mathrm{g})} = K_B \bullet \frac{n_0(NH_3 \bullet H_2O) - n(NH_3,g)}{n_0(NH_3 \bullet H_2O) - n(NH_3,g) + \frac{v(H_2O) \bullet \rho(H_2O)}{M(H_2O)}} \tag{6}$$

Where $P(\mathrm{NH_3,g})$ is partial pressure of gaseous ammonia, K_B is Henry's constant 0.297 Pa(H_2O in Water, 298.15 K), $n(\mathrm{NH_3,g})$ is the amount of ammonia in the gaseous state, $n_0(\mathrm{NH_3{\cdot}H_2O})$ is the amount of ammonia in the H_2O in the initial state, n $(\mathrm{NH_3},\ g)$ is the amount of ammonia in the gaseous state in the current, $v(\mathrm{H_2O})$ is volume of water, $\rho(\mathrm{H_2O})$ is the density of water, $\mathrm{M(H_2O)}$ is Molar mass of water H_2O.

2.6. Use of fluorescent paper-based sensor to detect chicken breast sample freshness

Fresh chicken breast weighing 30 g was placed in a single-use plastic container. The fluorescent sensor made of paper was positioned at the bottom of the box and kept at 4 °C. Every 24 h, sensor fluorescence images were captured.

3. Results and discussions

3.1. Complex structural analysis

Zinc metal complexes have a strong absorption peak between 350 nm ~ 400 nm, and under the excitation peak of 365 nm wavelength, the complex has a weak emission peak at 540 nm. According to Fig. 2(a) Two emission peaks can be observed at the excitation wavelength at 365 nm. The emission peak at 440 nm is the characteristic peak emitted by CNQDs, while the emission peak at 540 nm is the characteristic peak emitted by the Zn complex. As can be seen from the SEM diagram (Fig. 2 (b)), Zn(PA)(BPE) appears blocky, while according to TEM, CNQDs are adsorbed on the surface of Zn(PA)(BPE) (Fig. 2(c)). According to the

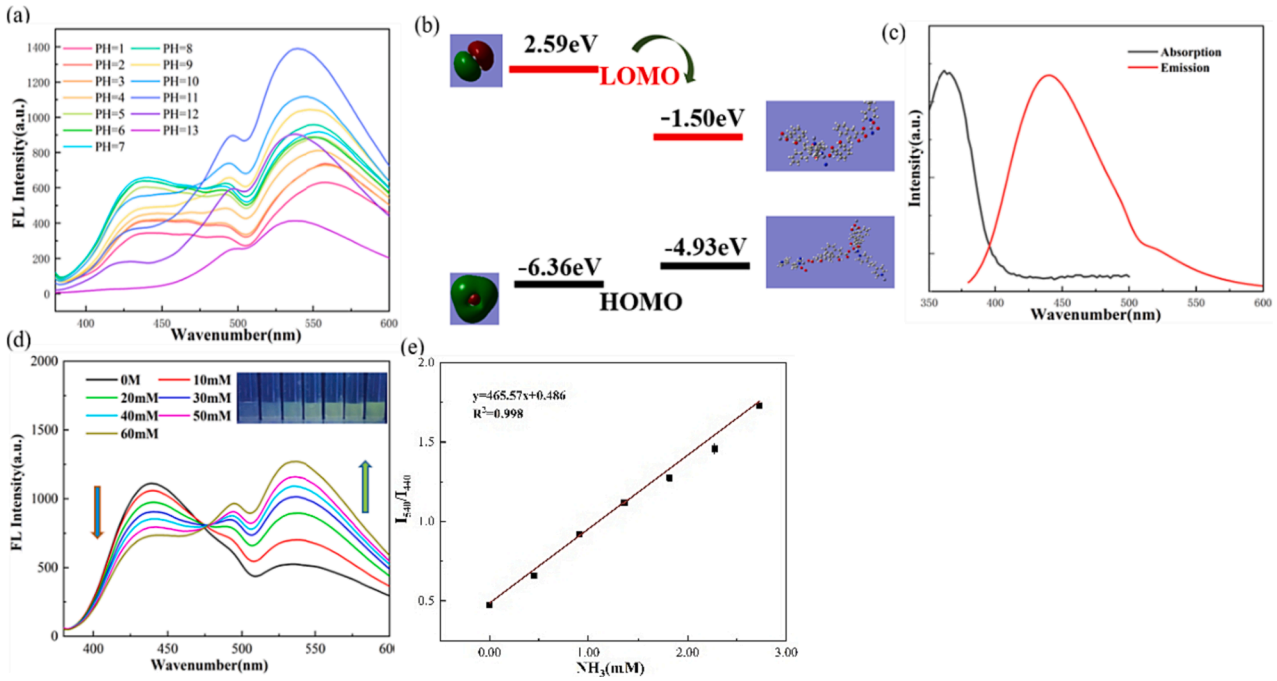

Fig. 4. (a) Fluorescence intensity of complexes at different pH; (b) HOMO and LOMO energy level orbits of complexes and ammonia; (c) CDs emission spectra and Zn (PA)(BPE) absorption spectra; (d) Fluorescence intensity change of complex at 0 ~ 50 mM ammonia concentration; (e) Standard curve between ammonia concentration and fluorescence intensity ratio.

electron microscopy diagram, we preliminarily obtained the Zn metal complex and CNQDs combined complex. As shown in potential diagram (Fig. 2(d)), the Zn(PA)(BPE) has a positive charge on the surface, while CNQDs have a negative charge on the surface. Therefore, under the action of physical conditions, positively-charged Zn(PA)(BPE) and negatively-charged CNQDs were adsorbed together by electrostatic action. The infrared spectrum of the complex (Fig. 2(e)) was also observed, with the characteristic peaks of the infrared spectrum of both CNQDs and Zn complexes. For CNQDs, the peaks at 1406 cm^{-1} are assigned to stretching modes of C—N heterocycles. For CPs, the sharp absorption peak at 810 cm^{-1} was attributed to the ring bending vibration modes that are characteristic of C—O. The other peaks present in 1456 cm^{-1} and 1374 cm^{-1} correspond to the typical stretching vibration modes of C—N heterocycles. For the compound, the peak at 3200–3000 cm^{-1} is assigned to O—H and N—H stretching (Mani, Ojha, Reddy, & Mandal, 2017), although the two elastic stretching vibration peaks mostly overlap, subtle differences can still be observed, thus inferring that the complex has the surface structure of the two substances.

3.2. Analysis of optical properties of complexes

The optical signal of the complex at different pH was further studied. Prior to proceeding, the complex concentration was optimized to ensure maximum response of the optical signal during the complex reaction. According to Fig. 3, different concentrations of complexes undergo different degrees of fluorescence enhancement after reacting with 0.1 M ammonia. As shown in Fig. 3 (a) when the concentration of the complex was 1.5 mg/ml, the fluorescence inner filter effect occurs after the complex reacts with ammonia, resulting in a decrease in fluorescence, while the low concentration of the complex result in a low fluorescence enhancement effect and a weak visualization effect, in Fig. 3 (h). The concentration of 3×10^{-2} mg/ml was selected for the study of the optical properties of the complex, and at this concentration, the complex had an obvious fluorescence enhancement effect.

3.3. Sensitivity and selectivity analysis of complex detection of ammonia

In order to investigate the fluorescence characteristics of the complex at different pH, this study measured the fluorescence enhancement intensity of a certain concentration of Zn (PA) @ CNQDs complex at different pH. According to Fig. 4(a), in strong acidic and alkaline environments, the fluorescence intensity of the composite decreases significantly at 540 nm, while in certain alkaline environments, the fluorescence intensity of the composite at this location is greatly enhanced. This indicates that alkaline environments can lead to an increase in the fluorescence intensity of the complex, but the intensity of fluorescence enhancement is not determined by the size of alkalinity. Similarly, the effect of different concentrations of ammonia solution on the fluorescence intensity of the composite was investigated in this study, as demonstrated in Fig. 4(a). The composite has two emission wavelengths of 440 nm and 540 nm at an excitation wavelength of 365 nm. With the addition of various ammonia aqueous solution concentrations, the emission peak at 540 nm gradually increased and the emission peak at 440 nm gradually decreased. To further explore the mechanism of the influence of ammonia on the fluorescence of the complex, Guassian software was used to calculate the LOMO and HOMO orbital energy levels of the complex and ammonia (Fig. 4(b)). Complex structure was optimized by density functional theory (DFT) and theoretical values were calculated using B3LYP/6-31G basis groups. From the Fig. 4(b), the LOMO orbitals of the complex were located between the ammonia level orbitals, and previous studies have known that fluorescence is enhanced when the LOMO orbitals of fluorescent material are between the energy level orbitals of the analyte (Jiang, Feng, Wang, Gu, Wei, Chen, et al., 2013). Therefore, it indicates the electrons in the ammonia are transferred to the orbital in the complex, resulting in enhanced fluorescence. At the same time, the emission peaks of CDs overlap to a certain extent with the absorption peaks of the complex (Fig. 4(c)), and according to the FRET effect, the emission peak at 440 nm weakens with the enhancement of 540 nm (Huang, Zhang, Huo, & Yin, 2021) (Fig. 4(d)). In the range of ammonia concentration from 0 to 3 mM, the intensity of I540/I440 is positively correlated with ammonia concentration, the correlation coefficient is 0.996, and the detection

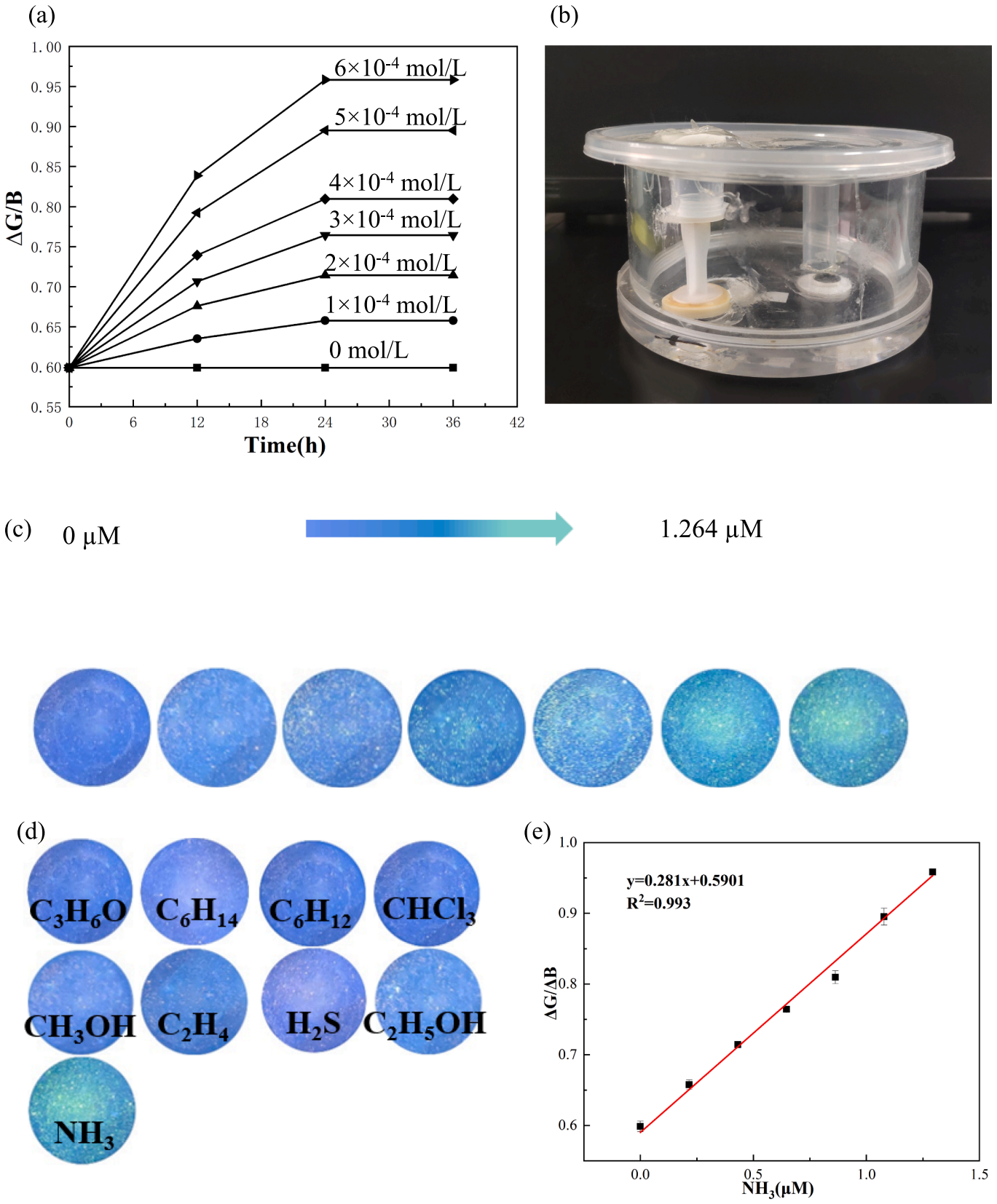

Fig. 5. (a) Sensor fluorescence intensity over time at different ammonia concentrations; (b) Ammonia gas reactor; (c) Sensor fluorescence change diagram in the range of 0 ~ 1.29356 μM ammonia concentration; (d) Changes in fluorescence intensity of sensors in different volatile gas environments (5 μM); (e) Standard curve between ammonia concentration and sensor △G/B.

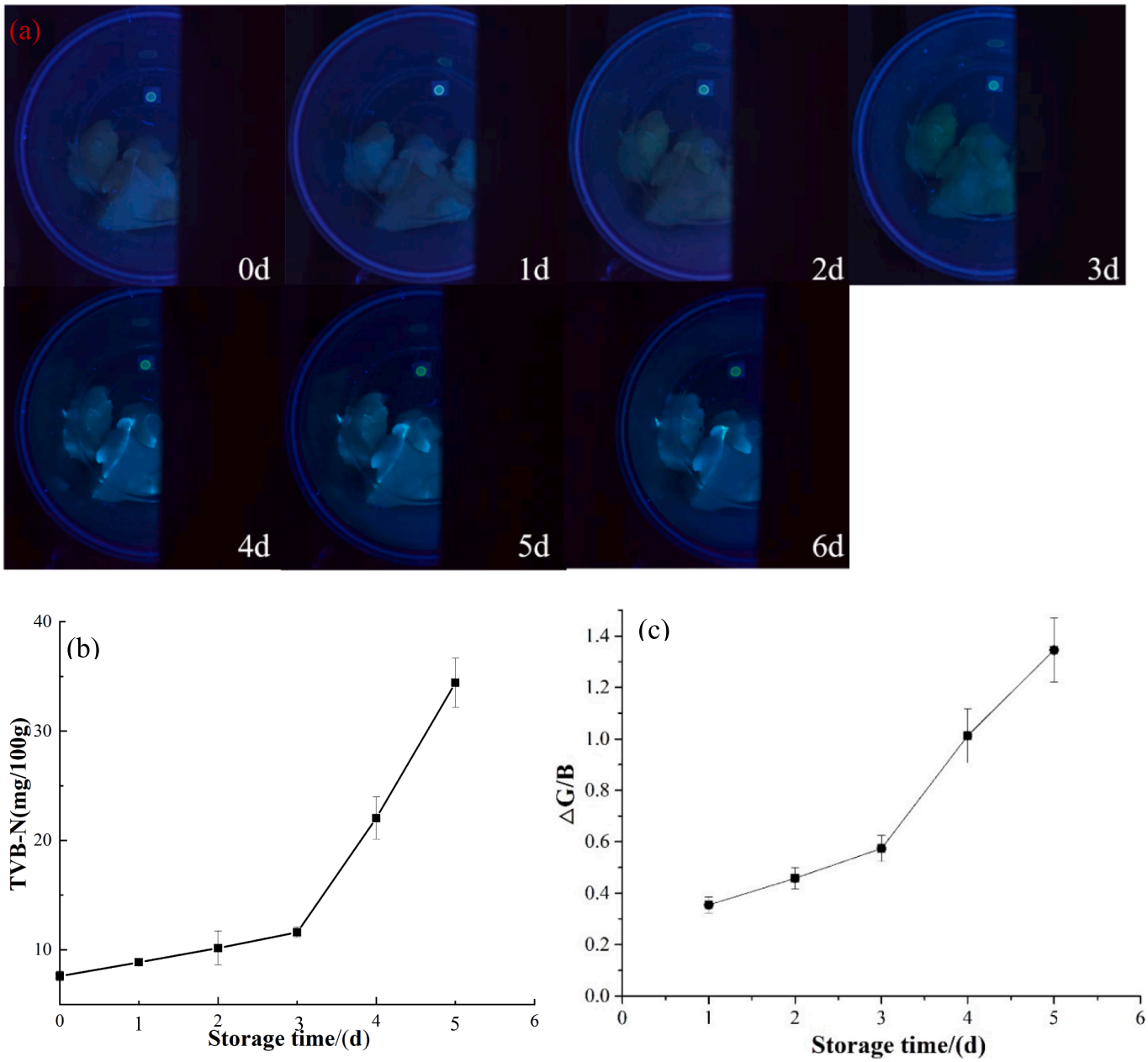

Fig. 6. Color evolution of composite fluorescence paper-based sensors to monitor fresh chicken breast deterioration at 4 °C, (b) TVB-N content in chicken breast at 4 °C and (c) Δ*G/B* values of the fluorescence paper-based sensors used to monitor fresh chicken breast spoilage at 4 °C.

limit is 10.4 μM calculated according to the signal-to-noise ratio of 3:1 (Fig. 4(e)). Compared with other studies for the detection of ammonia, this experiment has certain detection advantages (Table S1).

3.4. Construction of a portable ratiometric fluorescence sensor for ammonia detection

Inspired by the results of the reaction of the complex to an aqueous ammonia solution, this study further attempts to prepare a fluorescent paper-based sensor for detecting ammonia gas. Various volatile substances are produced during the spoilage process of chicken breast, among which ammonia and amine substances are the main characteristic spoilage gases. As shown in Fig. 5 (a), the fluorescence intensity of the sensor no longer changes after being exposed to the same environment as liquid ammonia for 24 h. Also, under the blank sample, the fluorescence intensity of the sensor did not change significantly. Therefore, the sensor has good stability in this environment. Therefore, we believe that the sensor can complete the detection after 24 h in a certain concentration of ammonia. To explore the sensing detection limit of solid-state sensors for ammonia, different concentrations of ammonia were placed with the sensor in a sealed reaction device (Fig. 5 (b)), and after waiting for a period of time, the change of its RGB value was obtained through the smartphone image and analysis (Fig. 5(c)). As shown in the figure, to explore the anti-interference of this sensor, some volatile components (such as hydrogen sulfide, acetone, hexane, cyclohexane, trichloroethane, ethylene, isopropanol, and methanol) were selected to test, as can be observed from the Fig. 5(d), the composite sensor has some ammonia selectivity. By correlating the obtained RGB value with the ammonia concentration, it concludes that in the range of ammonia gas concentration 0 ~ 1.296 μM, the detection limit of the solid sensor is 288 nM, and the sensor has good detection sensitivity and selectivity (Fig. 5(e)). The specific concentration of ammonia in the gas phase is obtained by Henry's law (the *eq*. (6).

3.5. Application of solid-state sensor in chicken breast freshness detection process

In order to detect the fluorescence change of the sensor during the chicken breast spoilage process, the fluorescence paper-based sensors were placed with the chicken breast in a same box at 4 °C to observe the fluorescence change (Fig. 6(a)). The sensor was photographed every 24 h to analyze the change of the sensor RGB value with storage time. The relationship between the change in sensor fluorescence and the freshness of chicken breast was analyzed. At the same time, the Kjeldahl method was used to calculate the TVB-N content of chicken breast every 24 h. In the first three days, the TVB-N concentration were no more than 15 mg/100 g (Fig. 6(b)). It is mean that the chicken breast is fresh and the $\Delta G/B$ value of fluorescence paper-based sensors was less than 0.6 (Fig. 6(c)). 4 days later, the TVBN level was above 20 mg/100 g, the fluorescent paper-based sensors' $\Delta G/B$ value climbed to 1.0 because the chicken breast was not fresh.. An increase in $\Delta G/B$ value above 1.0 demonstrates that the membrane's color has altered and entered a different color space, as demonstrated in Fig. 6(b). In contrast to chemical detection techniques, the fluorescence paper-based sensor in terms of sensitivity, the connections between the TVB-N concentration and the $\Delta G/B$ values were established:

$$y_{(\mathrm{lgTVB\text{-}N})} = -0.0542x^2 + 0.984x - 1.0774 \; R^2 = 0.981 \quad (7)$$

where the y is concentration of TVB-N, x is ΔG/B values.

The data analysis revealed that the fluorescence paper-based sensor's G/B value can accurately considering the chemical quality parameters of chicken breast, particularly when those indications include volatile components that are typical. The anticipated correlation rate was more than 0.98. The $\Delta G/B$ value of fluorescence paper-based sensor can deliver real-time information regarding the condition of the chicken breast to users (manufacturers, merchants, and consumers).

4. Conclusion

In order to develop an anti-interference, intuitive and sensitive intelligent label for monitoring the freshness of chicken breast, a ratio fluorescent ammonia gas sensor was constructed in this study. Firstly, the two fluorescent materials CNQDs and Zn(PA)(BPE) utilize electrostatic interaction to form a relatively stable complex. The complex is excited at 365 nm excitation wavelength, the fluorescence of the complex gradually changes from blue to green as the concentration of ammonia increases. This fluorescence probe can detect NH_3 in liquid phase with a linear range of 0–3 mM and LOD value of 10.4 μM. Secondly, in order to judge the freshness of the chicken breast, the compound was prepared into a fluorescence paper-based sensors to detect the ammonia in gaseous phase, and LOD value was 288 nM. The fluorescence paper-based sensors were successfully employed as a low-cost, high sensitivity and NH_3 quick-responsive intelligent tagging system for real-time monitoring of the chicken breast freshness, which was verified with the standard food-monitoring methods, TVB-N. The correlations between the TVB-N concentration and the ΔG/B values of the fluorescence paper-based sensors were also established, over 0.98 was the predictive correlation coefficient. These fluorescence paper-based sensors are of great significance for ensuring food safety, which have great practical application value in food industry.

Ethical Approval

This article does not contain any studies with human participants or animals performed by any of the authors.

CRediT authorship contribution statement

Huang Xiaowei: Conceptualization, Methodology. **Zhao Wanying:** Writing – original draft. **Sun Wei:** Methodology. **Li Zhihua:** Supervision, Funding acquisition, Writing – review & editing. **Zhang Ning:** Validation, Investigation. **Shi Jiyong:** Validation. **Zhang Yang:** Data curation. **Zhang Xinai:** Resources. **Shen Tingting:** Data curation. **Zou Xiaobo:** Supervision.

Declaration of competing interest

The authors declare that they have no known competing financial interests or personal relationships that could have appeared to influence the work reported in this paper.

Data availability

Data will be made available on request.

Acknowledgement

The National key research and development plan (2023YFE0105500), National Natural Science Foundation of China (grant numbers 32272407), Jiangsu Natural Science Foundation for Excellent Young Scholars (grant numbers BK20200103, BK20220111), China Postdoctoral Science Foundation (grant number 2020M683372), Natural Science Foundation of Jiangsu Province (grant number BE2022313, BK20220058), Jiangsu Specially-Appointed Professor (grant number 202074), Earmarked Fund for China Agriculture Research System (grant number CARS-27).

Appendix A. Supplementary data

Supplementary data to this article can be found online at https://doi.org/10.1016/j.fochx.2023.101054.

References

Cai, S. Y., Song, G. J., Zhang, G. F., Wang, L., Jian, T. L., Xu, J. T., … Tian, Y. Q. (2022). A multicolor fluorescent sensor array based on curcumin and its analogs as a shrimp freshness indicator. *Sensors and Actuators B-Chemical, 367*.

Chen, L., Ding, H., Zhu, Y. L., Guo, Y. W., Tang, Y. Y., Xie, K. Z., … Zhang, T. (2023). Untargeted and targeted metabolomics identify metabolite biomarkers for Salmonella enteritidis in chicken meat. *Food Chemistry, 409*, Article 135294.

Huang, Y., Zhang, Y., Huo, F., & Yin, C. (2021). FRET-dependent single/two-channel switch endowing a dual detection for sulfite and its organelle targeting applications. *Dyes and Pigments, 184*, Article 108869.

Jia, R., Tian, W., Bai, H., Zhang, J., Wang, S., & Zhang, J. (2019). Amine-responsive cellulose-based ratiometric fluorescent materials for real-time and visual detection of shrimp and crab freshness. *Nature Communications, 10*(1), 795.

Jia, Z., Luo, Y., Wang, D., Dinh, Q. N., Lin, S., Sharma, A., … Pearlstein, A. J. (2021). Nondestructive multiplex detection of foodborne pathogens with background microflora and symbiosis using a paper chromogenic array and advanced neural network. *Biosensors & Bioelectronics, 183*, Article 113209.

Jiang, H. L., Feng, D., Wang, K., Gu, Z. Y., Wei, Z., Chen, Y. P., & Zhou, H. C. (2013). An exceptionally stable, porphyrinic Zr metal-organic framework exhibiting pH-dependent fluorescence. *Journal of the American Chemical Society, 135*(37), 13934–13938.

Jiao, W., Sun, X. Y., Hui, Z., Dong, M. N., Li, L. H., Hui, Z. S., & Li, W. (2022). Dual-functional intelligent gelatin based packaging film for maintaining and monitoring the shrimp freshness. *Food Hydrocolloids, 124*.

Kim, Y. Y., Park, S. J., Kim, J. S., & Shin, H. S. (2022). Development of freshness indicator for monitoring chicken breast quality and freshness during storage. *Food Science and Biotechnology, 31*(3), 377–385.

Kuswandi, B., Jayus, Oktaviana, R., Abdullah, A., & Heng, L. Y. (2014). A Novel On-Package Sticker Sensor Based on Methyl Red for Real-Time Monitoring of Broiler Chicken Cut Freshness. *Packaging Technology and Science, 27*(1), 69–81.

Lee, K., Baek, S., Kim, D., & Seo, J. (2019). A freshness indicator for monitoring chicken-breast spoilage using a Tyvek (R) sheet and RGB color analysis. *Food Packaging and Shelf Life, 19*, 40–46.

Lee, K., Park, H., Baek, S., Han, S., Kim, D., Chung, S., … Seo, J. (2019). Colorimetric array freshness indicator and digital color processing for monitoring the freshness of packaged chicken breast. *Food Packaging and Shelf Life, 22*, Article 100408.

Li, P. Y., Rao, D. M., Wang, Y. M., & Hu, X. R. (2022). Adsorption characteristics of polythiophene for tetracyclines and determination of tetracyclines in fish and chicken manure by solid phase extraction-HPLC method. *Microchemical Journal, 173*, Article 106935.

Li, W. Y., Sun, L., Liu, C. L., Rotaru, A., Robeyns, K., Singleton, M. L., & Garcia, Y. (2022). Supramolecular FeII4L4 cage for fast ammonia sensing. *Journal of Materials Chemistry C, 10*(24), 9216–9221.

Lü, B., Chen, Y., Li, P., Wang, B., Müllen, K., & Yin, M. (2019). Stable radical anions generated from a porous perylenediimide metal-organic framework for boosting near-infrared photothermal conversion. *Nature Communications, 10*(1), 767.

Lu, P., Yang, Y., Liu, R., Liu, X., Ma, J. X., Wu, M., & Wang, S. F. (2020). Preparation of sugarcane bagasse nanocellulose hydrogel as a colourimetric freshness indicator for intelligent food packaging. *Carbohydrate polymers, 249*, Article 116831.

Luo, J., Zhu, Z. H., Lv, W., Wu, J., Yang, J. H., Zeng, M., … Yang, Z. (2023). E-Nose System Based on Fourier Series for Gases Identification and Concentration Estimation From Food Spoilage. *IEEE Sensors Journal, 23*(4), 3342–3351.

Mallick, S., Chandra, F., & Koner, A. L. (2016). A ratiometric fluorescent probe for detection of biogenic primary amines with nanomolar sensitivity. *Analyst, 141*(3), 827–831.

Mani, P., Ojha, A. A., Reddy, V. S., & Mandal, S. (2017). "Turn-on" Fluorescence Sensing and Discriminative Detection of Aliphatic Amines Using a 5-Fold-Interpenetrated Coordination Polymer. *Inorganic Chemistry*, 6772–6775.

Mastnak, T., Mohr, G. J., & Finsgar, M. (2023). The use of a novel smartphone testing platform for the development of colorimetric sensor receptors for food spoilage. *Analytical Methods, 15*(13), 1700–1712.

Meng, Y. H., Luo, H. Z., Dong, C. H., Zhang, C. L., He, Z. B., Long, Z., & Cha, R. T. (2020). Hydroxypropyl Guar/Cellulose Nanocrystal Film with Ionic Liquid and Anthocyanin for Real-Time and Visual Detection of NH3. *ACS Sustainable Chemistry & Engineering, 8*(26), 9731–9741.

Moosavi-Nasab, M., Khoshnoudi-Nia, S., Azimifar, Z., & Kamyab, S. (2021). Evaluation of the total volatile basic nitrogen (TVB-N) content in fish fillets using hyperspectral imaging coupled with deep learning neural network and meta-analysis. *Scientific Reports, 11*(1), 5094.

Qin, Y. Q., Ke, W. K., Faheem, A., Ye, Y. Y., & Hu, Y. G. (2023). A rapid and naked-eye on-site monitoring of biogenic amines in foods spoilage. *Food Chemistry, 404*, Article 134581.

Rosniawati, T., Rahayu, W. P., Kusumaningrum, H. D., Indrotristanto, N., & Nikastri, E. (2021). Prevalence and level of Salmonella spp. Contamination on selected pathways of preparation and cooking of fried chicken at the household level. *Food Science and Technology, 41*, 41–46.

Sun, L., Rotaru, A., & Garcia, Y. (2022). A non-porous Fe(II) complex for the colorimetric detection of hazardous gases and the monitoring of meat freshness. *Journal of Hazardous Materials, 437*, Article 129364.

Sun, Y., Zhang, M., Adhikari, B., Devahastin, S., & Wang, H. (2022). Double-layer indicator films aided by BP-ANN-enabled freshness detection on packaged meat products. *Food Packaging and Shelf Life, 31*.

Wang, H., Cui, J., Arshad, A., Xu, S., & Wang, L. (2018). A visual photothermal paper sensor for H2S recognition through rational modulation LSPR wavelength of plasmonics. *Science China Chemistry, 61*(3), 368–374.

Wang, J., Li, D., Ye, Y., Qiu, Y., Liu, J., Huang, L., … Chen, B. (2021). A Fluorescent Metal-Organic Framework for Food Real-Time Visual Monitoring. *Adv Mater, 33*(15), e2008020.

Wojnowski, W., Namiesnik, J., & Plotka-Wasylka, J. (2019). Dispersive liquid-liquid microextraction combined with gas chromatography-mass spectrometry for in situ determination of biogenic amines in meat: Estimation of meat's freshness. *Microchemical Journal, 145*, 130–138.

Xiao, Q., Sui, H. L., Yu, Q., Chen, J., Yin, Y., & Ju, X. (2019). Gas Releasing Mechanism of LLM-105 Using Two-Dimensional Correlation Infrared Spectroscopy. *Propellants Explosives Pyrotechnics, 44*(11), 1375–1383.

Zhang, E. S., Hou, X. F., Yang, H., Zou, Y., & Ju, P. (2020). A novel bicoumarin-based multifunctional fluorescent probe for naked-eye sensing of amines/ammonia. *Analytical Methods, 12*(13), 1744–1751.

Zhang, J., Xu, Z., Shi, C., & Yang, X. (2021). A Fluorescence Method Based on N, S-Doped Carbon Dots for Detection of Ammonia in Aquaculture Water and Freshness of Fish. *Sustainability, 13*.